Adaptive Subcarrier PSK Intensity Modulation in Free Space Optical Systems

Nestor D. Chatzidiamantis, *Student Member, IEEE,* Athanasios S. Lioumpas, George K. Karagiannidis, *Senior Member, IEEE,* and Shlomi Arnon, *Senior Member, IEEE*

***Abstract*—We propose an adaptive transmission technique for free space optical (FSO) systems, operating in atmospheric turbulence and employing subcarrier phase shift keying (S-PSK) intensity modulation. Exploiting the constant envelope characteristics of S-PSK, the proposed technique offers efficient utilization of the FSO channel capacity by adapting the modulation order of S-PSK, according to the instantaneous state of turbulence induced fading and a pre-defined bit error rate (BER) requirement. Novel expressions for the spectral efficiency and average BER of the proposed adaptive FSO system are presented and performance investigations under various turbulence conditions, turbulence models, and target BER requirements are carried out. Numerical results indicate that significant spectral efficiency gains are offered without increasing the transmitted average optical power or sacrificing BER requirements, especially in moderate-to-strong turbulence conditions. Furthermore, the proposed variable rate transmission technique is applied to multiple input multiple output (MIMO) FSO systems, providing additional improvement in the achieved spectral efficiency as the number of the transmit and/or receive apertures increases.**

***Index Terms*—Adaptive modulation, atmospheric turbulence, free-space optical communications, multiple input multiple output (MIMO), subcarrier PSK intensity modulation, variable rate.**

I. Introduction

FREE space optical (FSO) communication is a wireless technology, which has recently attracted considerable interest within the research community, since it can be advantageous for a variety of applications [1]–[3]. However, despite its significant advantages, the widespread deployment of FSO systems is limited by their high vulnerability to adverse atmospheric conditions [4]. Even in a clear sky, due to inhomogeneities in temperature and pressure changes, the refractive index of the atmosphere varies stochastically and results in atmospheric turbulence. This causes rapid fluctuations at the intensity of the received optical signal, known as turbulence-induced fading, that severely affects the reliability and/or communication rate provided by the FSO link.

Over the last years, several fading mitigation techniques have been proposed for deployment in FSO links to combat the degrading effects of atmospheric turbulence. Error control coding (ECC) in conjunction with interleaving has been investigated in [5] and [6]. Although this technique is known in the radio frequency (RF) literature to provide an effective time-diversity solution to rapidly-varying fading channels, its practical use in FSO links is limited due to the large-size interleavers[1] required to achieve the promising coding gains theoretically available. Maximum likelihood sequence detection (MLSD), which has been proposed in [7], efficiently exploits the channel's temporal characteristics; however it suffers from extreme computational complexity and therefore in practice, only suboptimal MLSD solutions can be employed [8]–[10]. Of particular interest is the application of spatial diversity to FSO systems, i.e., transmission and/or reception through multiple apertures, since significant performance gains are offered by taking advantage of the additional degrees of freedom in the spatial dimension [11], [12]. Nevertheless, increasing the number of apertures, increases the cost and the overall physical size of the FSO systems.

Another promising solution is the employment of adaptive transmission, a well known technique employed in RF systems [13], [14]. By varying basic transmission parameters according to the channel's fading intensity, adaptive transmission takes advantage of the time varying nature of turbulence, allowing higher data rates to be transmitted under favorable turbulence conditions. Thus, the spectral efficiency of the FSO link can be improved without wasting additional optical power or sacrificing performance requirements. The concept of adaptive transmission was first introduced in the context of FSO systems in [15], where an adaptive scheme that varied the period of the transmitted binary pulse position modulated (BPPM) symbol was studied. Since then, various adaptive FSO systems have been proposed. In [16], a variable rate FSO system employing adaptive Turbo-based coding schemes in conjunction with on-off keying modulation was investigated, while in [17] an adaptive power scheme was suggested for reducing the average power consumption in constant rate optical satellite-to-earth

Paper approved by J. Liu, the Editor for Free Space Optics and Hybrid RF/Optical Wireless Systems of the IEEE Communications Society. Manuscript received February 9, 2010; revised September 27, 2010.

This paper was partially presented at the IEEE Global Communications Conference (GLOBECOM'10).

N. D. Chatzidiamantis and G. K. Karagiannidis are with the Wireless Communications Systems Group (WCSG), Department of Electrical and Computer Engineering, Aristotle University of Thessaloniki, GR-54124 Thessaloniki, Greece (e-mail: {nestoras, geokarag}@auth.gr).

A. S. Lioumpas was with the Department of Electrical and Computer Engineering, Aristotle University of Thessaloniki, Greece. He is now with the Department of Digital Systems, University of Piraeus, Piraeus, Greece (e-mail: lioumpas@webmail.unipi.gr).

S. Arnon is with the Satellite and Wireless Communication Laboratory, Department of Electrical and Computer Engineering, Ben-Gurion University of the Negev, Beer-Sheva IL-84105, Israel (e-mail: shlomi@ee.bgu.ac.il).

Digital Object Identifier 10.1109/TCOMM.2011.022811.100078

[1]For the signalling rates of interest (typically of the the order of Gbps), FSO channels exhibit slow fading, since the correlation time of turbulence is of the order of 10^{-3} to 10^{-2} seconds.

links. Recently, in [18], an adaptive transmission scheme that varied both the power and the modulation order of a FSO system with pulse amplitude modulation (PAM), has been studied.

In this work, we propose an adaptive modulation scheme for FSO systems operating in turbulence, using an alternative type of modulation; subcarrier phase shift keying intensity modulation (S-PSK). S-PSK refers to the transmission of PSK modulated RF signals, after being properly biased[2], through intensity modulation direct detection (IM/DD) optical systems and its employment can be advantageous, since:

- in the presence of turbulence, it offers increased demodulation performance compared to PAM signalling [19]–[21],
- due to its constant envelope characteristic, both the average and peak optical power are constant in every symbol transmitted, and,
- it allows RF signals to be directly transmitted through FSO links providing protocol transparency in heterogeneous wireless networks [22]–[24].

Taking into consideration that the bias signal required by S-PSK in order to satisfy the non-negativity requirement is independent of the modulation order, we present a novel variable rate transmission strategy that is implemented through the modification of the modulation order of S-PSK, according to the instantaneous turbulence induced fading and a predefined value of Bit Error Rate (BER). The performance of the proposed variable rate transmission scheme is investigated, in terms of spectral efficiency and BER, under different degrees of turbulence strength and for different fading models, and is further compared to non-adaptive modulation and the upper channel capacity bound provided by [25]. Moreover, an application to multiple input multiple output (MIMO) FSO systems employing equal gain combining (EGC) at the receiver is provided and the performance of the presented transmission policy is evaluated for various MIMO deployments.

The remainder of the paper is organized as follows. In Section II, the non-adaptive S-PSK FSO system model is described and its performance in the presence of turbulence induced fading is investigated. In section III, the adaptive S-PSK strategy is presented, deriving expressions for its spectral efficiency and BER performance, and an application to MIMO FSO systems is further provided. Section IV discusses some numerical results and useful concluding remarks are drawn in section V.

II. Non-Adaptive Subcarrier PSK Intensity Modulation

We consider an IM/DD FSO system which uses a subcarrier signal for the modulation of the optical carrier's intensity and operates over the atmospheric turbulence induced fading channel.

A. System Model

1) Received Signal Model: At the transmitter end, we assume that the RF subcarrier signal is modulated by the data sequence using PSK. Moreover a proper DC bias is added in order to ensure that the transmitted waveform always satisfies the non-negativity input constraint. Hence, the transmitted optical power can be expressed as

$$P_t(t) = P[1 + \mu s(t)] \tag{1}$$

where P is the average transmitted optical power and μ is the modulation index $(0 < \mu < 1)$ which ensures that the laser operates in its linear region and avoids over-modulation induced clipping. Further, $s(t)$ is the output of the electrical PSK modulator which can be written as

$$s(t) = \sum_k g(t - kT)\cos(2\pi f_c t + \phi_k) \tag{2}$$

where f_c is the frequency of the RF subcarrier signal, T is the symbol's period, $g(t)$ is the shaping pulse, $\phi_k \in \left[0, ..., (M-1)\frac{\pi}{M}\right]$ is the phase of the kth transmitted symbol and M is the modulation order.

At the receiver's end, the optical power which is incident on the photodetector is converted into an electrical signal through direct detection. We assume operation in the high signal-to-noise ratio (SNR) regime where the shot noise caused by ambient light is dominant and therefore Gaussian noise model is used as a good approximation of the Poisson photon counting detection model [7].

After removing the DC bias and demodulating through an electrical PSK demodulator [21], the sampled electrical signal obtained at the output of the receiver, during the kth symbol interval, is expressed as

$$r[k] = \mu\eta\sqrt{\frac{E_g}{2}} P I[k]\, s[k] + n[k] \tag{3}$$

where η corresponds to the receiver's optical-to-electrical efficiency, $s[k] = \cos\phi_k - j\sin\phi_k$, E_g is the energy of the shaping pulse and $n[k]$ is the zero mean circularly symmetric complex Gaussian noise component with $\mathbb{E}\{n[k]\, n^*[k]\} = 2\sigma_n^2 = N_o$ and $\mathbb{E}\{\cdot\}$ denoting statistical expectation. Furthermore, $I[k]$ represents the turbulence-induced fading coefficient during the kth symbol interval.

Atmospheric turbulence results in a very slowly-varying fading in FSO systems. For the signalling rates of interest ranging from hundreds to thousands of Mbps [26], the fading coefficient can be considered constant over hundred of thousand or millions of consecutive symbols, since the coherence time of the channel is about 1-100ms [27]. Hence, it is assumed that turbulence induced fading remains constant over a block of K symbols (block fading channel), and therefore we drop the time index k, i.e.

$$I = I[k], \quad k = 1, ...K \tag{4}$$

It should be noted that in the analysis that follows, it is further assumed that the information message is long enough to reveal the long-term ergodic properties of the turbulence process.

The instantaneous electrical SNR is defined as

$$\gamma = \frac{\mu^2\eta^2 P^2 E_s I^2}{N_o} \tag{5}$$

while the average electrical SNR is given by

$$\bar{\gamma} = \frac{\mu^2\eta^2 P^2 E_s}{N_o} \tag{6}$$

[2]Since optical intensity must satisfy the non-negativity constraint, a proper DC bias must be added to the RF electrical signal in order to prevent clipping and distortion in the optical domain.

with $E_s = \frac{E_g}{2}$.

2) Atmospheric Turbulence Models: Atmospheric turbulence is a major performance-degrading factor in FSO systems, which leads to intensity variations of the received optical signals. For its statistical description, various statistical models have been proposed in the literature [1], depending on the turbulence strength. The scintillation index, defined as [1]

$$\sigma_I^2 \triangleq \frac{\mathbb{E}\left\{I^2\right\}}{\left(\mathbb{E}\left\{I\right\}\right)^2} - 1 \tag{7}$$

is a measure of the turbulence strength. Lower values of scintillation index lead to less intensity variations, while higher values result in more severe turbulence-induced fading. Moreover, without loss of generality, it is assumed that the mean of the intensity variations is normalized, i.e. $\mathbb{E}\left\{I\right\} = 1$.

In weak turbulence conditions $\left(\sigma_I^2 < 0.5\right)$, the most widely accepted fading model is the lognormal (LN) one. In this case, the logarithm of the intensity variations is normally distributed, according to [11], [27]

$$I = \exp\left(2x\right) \tag{8}$$

where x is a normally distributed random variable with mean m_x and variance σ_x^2, i.e., its probability density function (PDF) is $f_x\left(x\right) = \mathcal{N}\left(m_x, \sigma_x^2\right)$. Hence, I follows a lognormal distribution with PDF provided by

$$f_I\left(I\right) = \frac{1}{2I}\frac{1}{\sqrt{2\pi\sigma_x^2}}\exp\left(-\frac{\left(\ln I - 2m_x\right)^2}{8\sigma_x^2}\right) \tag{9}$$

with $m_x = -\sigma_x^2$, since $\mathbb{E}\left\{I\right\} = 1$. The scintillation index is calculated according to $\sigma_I^2 = \exp\left(4\sigma_x^2\right) - 1$.

In moderate to strong turbulence conditions, the recently proposed Gamma-Gamma (GG) model can be used for the statistical description of turbulence-induced fading. According to this model, intensity fluctuations are considered to be derived from the product of small-scale and large-scale fluctuations, both statistically defined by the Gamma distribution. Hence, in this case, the PDF of the intensity variations is given by [1], [28]

$$f_I\left(I\right) = \frac{2\left(\alpha\beta\right)^{\frac{\alpha+\beta}{2}}}{\Gamma\left(\alpha\right)\Gamma\left(\beta\right)} I^{\frac{\alpha+\beta-2}{2}} K_{\alpha-\beta}\left(2\sqrt{\alpha\beta I}\right) \tag{10}$$

where $\Gamma\left(\cdot\right)$ is the gamma function [29, Eq. (8.310)], $K_\nu\left(\cdot\right)$ is the νth order modified Bessel function of the second kind [29, Eq. (8.432/9)], and α and β are the parameters which are related with effective atmospheric conditions [1]. The scintillation index is calculated according to $\sigma_I^2 = \alpha^{-1} + \beta^{-1} + \left(\alpha\beta\right)^{-1}$.

B. BER Performance

The BER performance of the non-adaptive S-PSK FSO system depends on the statistics of the atmospheric turbulence and the modulation order. Specifically, the conditioned on the fading coefficient, I, BER is given by [21], [30]

$$P_b\left(M, I\right) = AQ\left(I\sqrt{2\bar{\gamma}}B\right) \tag{11}$$

where $A = 1$ and $B = 1$ when $M = 2$, $A = \frac{2}{\log_2 M}$ and $B = \sin\frac{\pi}{M}$ when $M > 2$. Further $Q\left(\cdot\right)$ is the Gaussian Q-function defined as $Q\left(x\right) = \frac{1}{\sqrt{2\pi}}\int_x^\infty e^{-\frac{t^2}{2}}dt$. Hence, the average BER will be obtained by averaging (11) over the turbulence PDF, i.e.,

$$\bar{P}_b\left(M\right) = \int_0^\infty P_b\left(M, I\right) f_I\left(I\right) dI. \tag{12}$$

Corollary 1: The average BER of the non-adaptive S-PSK FSO system in LN turbulence induced fading can be numerically computed by

$$\bar{P}_b\left(M\right) \approx \frac{A}{\sqrt{\pi}}\sum_{i=1}^{k} w_i Q\left(\sqrt{2\bar{\gamma}}B\exp\left(2\sqrt{2}\sigma_x z_i - 2\sigma_x^2\right)\right) \tag{13}$$

where k is the order of approximation, z_i, $i = 1, ..., k$, are the zeros of the kth order Hermite polynomial, $H_k\left(z\right)$, and $w_i = \frac{2^{k-1}k!\sqrt{\pi}}{k^2\left[H_{k-1}\left(w_i\right)\right]^2}$, $i = 1, ..., k$, are the weight factors for the kth order approximation.

Proof: Using (8) and (9), (12) can be equivalently written as

$$\bar{P}_b\left(M\right) = \frac{A}{\sqrt{2\pi\sigma_x^2}} \times \int_{-\infty}^{\infty}\exp\left(-\frac{\left(x+\sigma_x^2\right)}{2\sigma_x^2}\right) Q\left(\sqrt{2\bar{\gamma}}B\exp\left(2x\right)\right) dx \tag{14}$$

By applying the transformation $y = \frac{x+\sigma_x^2}{\sqrt{2\sigma_x^2}}$ and using the Gauss-Hermite quadrature formula [31, Eq. (25.4.46)], (14) can be numerically calculated by (13). ■

Corollary 2: The average BER of the non-adaptive S-PSK FSO system in GG turbulence induced fading is analytically evaluated by

$$\bar{P}_b\left(M\right) = \frac{2^{\alpha+\beta-3}A}{\Gamma\left(\alpha\right)\Gamma\left(\beta\right)\pi^{\frac{3}{2}}} G_{2,5}^{4,2}\left[\frac{\left(\alpha\beta\right)^2}{16\bar{\gamma}B^2}\,\middle|\,\begin{matrix}\frac{1}{2}, 1\\ \frac{\alpha}{2}, \frac{\alpha+1}{2}, \frac{\beta}{2}, \frac{\beta+1}{2}, 0\end{matrix}\right] \tag{15}$$

where $G_{p,q}^{m,n}\left[\cdot\right]$ is the Meijer's G-function [29, Vol. 3, Eq. (9.301)].

Proof: Using (10) and an alternative representation of the Q-function, $Q\left(x\right) = \frac{1}{2}\mathrm{erfc}\left(\frac{x}{\sqrt{2}}\right)$ where $\mathrm{erfc}\left(\cdot\right)$ is the complementary error function, (12) can be equivalently written as

$$\bar{P}_b\left(M\right) = \frac{\left(\alpha\beta\right)^{\frac{\alpha+\beta}{2}}A}{\Gamma\left(\alpha\right)\Gamma\left(\beta\right)} \times \int_0^\infty I^{\frac{\alpha+\beta}{2}-1} K_{\alpha-\beta}\left(2\sqrt{\alpha\beta I}\right)\mathrm{erfc}\left(\sqrt{\bar{\gamma}}BI\right) dI \tag{16}$$

By expressing the integrands of (16) in terms of Meijer's G-functions, according to [32, Vol. 3, Eq. (8.4.14/2)] and [32, Vol. 3, Eq. (8.4.23/1)], and using [32, Vol. 3, Eq. (2.24.1/1)] along with [32, Vol. 3, Eq. (8.2.2/14)], the closed-form solution of (15) is yielded. ■

C. High-SNR Channel Capacity Upper Bound

Using the trigonometric moment space method, an upper bound for the capacity of optical intensity channels when multiple subcarrier modulation is employed, has been derived in [25]. By applying these results to the FSO system under

consideration (one subcarrier), the conditioned on the fading coefficient, I, channel capacity can be upper bounded by

$$C_{up}(I) = \frac{W}{2}\left[\log_2 \pi + \log_2\left(\frac{\mu^2\eta^2 P^2 E_g I^2}{\pi e N_o}\right) + o(\sigma_n)\right] \tag{17}$$

where W denotes the electrical bandwidth and $o(\sigma_n)$ represents the capacity residue which vanishes exponentially as $\sigma_n \to 0$. Hence at high values of electrical SNR, (17) can be approximated by

$$C_{up}^{\infty}(I) = \frac{W}{2}\log_2\left(\frac{\bar{\gamma} I^2}{e}\right). \tag{18}$$

The unconditional high-SNR channel capacity upper bound, which will be used as a benchmark in the analysis that follows, is obtained by averaging (18) over the fading distribution, i.e.,

$$C_{up}^{\infty} = \frac{W}{2}\int_0^{\infty}\log_2\left(\frac{\bar{\gamma} I^2}{e}\right) f_I(I)\, dI. \tag{19}$$

Corollary 3: The high-SNR channel capacity upper bound in LN turbulence induced fading is given by

$$C_{up}^{\infty} = \frac{W}{2}\left[\log_2\left(\frac{\bar{\gamma}}{e}\right) - \frac{4\sigma_x^2}{\ln 2}\right]. \tag{20}$$

Proof: A detailed proof is provided in Appendix. ∎

Corollary 4: The high-SNR channel capacity upper bound in GG turbulence induced fading is given by

$$C_{up}^{\infty} = \frac{W}{2}\log_2\left(\frac{\bar{\gamma}}{e}\right) + \frac{W}{\ln 2}\left[\psi(\alpha) - \psi(\beta)\right] - W\log_2(\alpha\beta) \tag{21}$$

where $\psi(\cdot)$ is the Euler's digamma function [29, Eq. (8.360.1)].

Proof: Using (10), (21) can be written as

$$C_{up}^{\infty} = \frac{W}{2}\log_2\left(\frac{\bar{\gamma}}{e}\right) + \frac{2(\alpha\beta)^{\frac{\alpha+\beta}{2}} W}{\Gamma(\alpha)\Gamma(\beta)} \times \int_0^{\infty} I^{\frac{\alpha+\beta-2}{2}}\log_2 I K_{a-\beta}\left(2\sqrt{\alpha\beta I}\right) dI \tag{22}$$

which, after some basic algebraic manipulations and using [32, Vol. 2, Eq. (2.16.20.1)], is reduced to (21). ∎

III. Adaptive Modulation Strategy

In this section we introduce an adaptive modulation strategy that improves the spectral efficiency of S-PSK FSO systems, without increasing the transmitted average optical power or sacrificing the performance requirements.

A. Mode of Operation

By inserting pilot symbols at the beginning of a block of symbols[3], the receiver accurately estimates the instantaneous channel's fading state, I, which is experienced by the remaining symbols of the block. Based on this estimation, a decision device at the receiver selects the modulation order to be used for transmitting the non-pilot symbols of the block, configures the electrical demodulator accordingly and informs the adaptive PSK transmitter about that decision via a reliable RF feed back path.

The objective of the above described transmission technique is to maximize the number of bits transmitted per symbol interval, by using the largest possible modulation order under the target BER requirement P_o. Hence the problem is formulated as

$$\begin{aligned} &\max_{M} \ \log_2 M \\ &\text{s.t. } P_b(M, I) \le P_o \end{aligned} \tag{23}$$

In practice, the modulation order will be selected from N available ones, i.e. $\{M_1, M_2, ..., M_N\}$, depending on the values of I and P_o. Specifically, the range of the values of the fading term is divided in $(N+1)$ regions and each region is associated with the modulation order, M_j, according to the rule

$$M = M_j = 2^j \text{ if } I_j \le I < I_{j+1},\ j = 1, ...N \tag{24}$$

The region boundaries $\{I_j\}$ are set to the required values of turbulence-induced fading required to achieve the target P_o. Hence, according to (11), $\{I_j\}$ are calculated as

$$I_1 = \sqrt{\frac{1}{2\bar{\gamma}}} Q^{-1}(P_o), \tag{25}$$

$$I_j = \frac{1}{\sin\frac{\pi}{M_j}}\sqrt{\frac{1}{2\bar{\gamma}}} Q^{-1}\left(\frac{\log_2 M_j}{2} P_o\right),\ j = 2, ...N \tag{26}$$

and

$$I_{N+1} = R, \tag{27}$$

where $R \to \infty$ and $Q^{-1}(\cdot)$ denotes the inverse Q-function, which is a standard built-in function in most of the well-known mathematical software packages. It should be noted that in the case of $I < I_1$, the transmission is stopped.

B. Performance Evaluation

1) Achievable Spectral Efficiency: The achievable spectral efficiency is defined as the data rate transmitted in a given bandwidth, and for the communication system under consideration is given by[4]

$$S = \frac{C}{W} = \frac{\bar{n}}{2} \tag{28}$$

with C representing the data rate used for transmission, measured in bit/s, and $\bar{n}$ the average number of transmitted bits. The average number of transmitted bits in the adaptive S-PSK scheme is obtained by

$$\bar{n} = \sum_{j=1}^{N} u_j \log_2 M_j \tag{29}$$

where

$$\begin{aligned} u_j &= \Pr\{I_j \le I < I_{j+1}\} \\ &= \int_{I_j}^{I_{j+1}} f_I(I)\, dI = F_I(I_{j+1}) - F_I(I_j) \end{aligned} \tag{30}$$

[3]Taking into consideration the length of a transmitting block of symbols, the insertion of pilot symbols will not cause significant overhead.

[4]Note that since the subcarrier PSK modulation requires twice the bandwidth than PAM signalling, the average number of bits transmitted in a symbol's interval will be divided by two.

and $F_I(\cdot)$ is the cumulative density function (CDF) of the turbulence induced fading. Hence, taking into consideration (24) and (30), (28) can be equivalently written as

$$S = \frac{\sum_{j=1}^{N} j\left[F_I\left(I_{j+1}\right) - F_I\left(I_j\right)\right]}{2} \tag{31}$$

which is reduced to

$$S = \frac{N - \sum_{j=1}^{N} F_I\left(I_j\right)}{2} \tag{32}$$

since $F_I\left(I_{N+1}\right) \to 1$, according to (27).

Corollary 5: The spectral efficiency of the adaptive S-PSK FSO system in LN turbulence induced fading is obtained by

$$S = \frac{\sum_{j=1}^{N} Q\left(x_j\right)}{2} \tag{33}$$

where $x_j = \frac{\ln(I_j)+2\sigma_x^2}{2\sigma_x}$.

Proof: We first recall that the CDF of the LN fading distribution is given by

$$F_I\left(I_{th}\right) = 1 - Q\left(\frac{\ln\left(I_{th}\right) + 2\sigma_x^2}{2\sigma_x}\right). \tag{34}$$

Thus, (32) will be written as

$$S = \frac{N - \sum_{j=1}^{N}\left[1 - Q\left(x_j\right)\right]}{2} \tag{35}$$

with $x_j = \frac{\ln(I_j)+2\sigma_x^2}{2\sigma_x}$, which is reduced, after some basic algebraic manipulations, to (33). ∎

Corollary 6: The spectral efficiency of the adaptive S-PSK FSO system in GG turbulence induced fading is obtained by

$$S = \frac{N}{2} - \frac{1}{2\Gamma\left(\alpha\right)\Gamma\left(\beta\right)} \sum_{j=1}^{N} G_{1,3}^{2,1}\left[\alpha\beta I_j \,\middle|\, \begin{matrix} 1 \\ \alpha, \beta, 0 \end{matrix}\right]. \tag{36}$$

Proof: The proof follows trivially by combining the CDF of the GG fading model, expressed using [33] and [32, Vol.3, Eq. (8.2.2.15)] as

$$F_I\left(I_{th}\right) = \frac{1}{\Gamma\left(\alpha\right)\Gamma\left(\beta\right)} G_{1,3}^{2,1}\left[\alpha\beta I_j \,\middle|\, \begin{matrix} 1 \\ \alpha, \beta, 0 \end{matrix}\right], \tag{37}$$

with (32). ∎

2) Average Bit Error Rate: The average BER of the proposed variable rate FSO system can be calculated as the ratio of the average number of bits in error over the total number of transmitted bits [13]. The average number of bits in error can be obtained by

$$\bar{n}_{err} = \sum_{j=1}^{N+1} \left\langle P_b \right\rangle_j \log_2 M_j \tag{38}$$

where

$$\left\langle P_b \right\rangle_j = \int_{I_j}^{I_{j+1}} P_b\left(M_j, I\right) f_I\left(I\right) dI \tag{39}$$

and can be evaluated only numerically for both fading models. Hence the average BER is given by

$$\bar{P}_b = \frac{\bar{n}_{err}}{\bar{n}}. \tag{40}$$

C. Application to MIMO FSO systems

Consider a Multiple Input Multiple Output (MIMO) FSO system where the information signal is transmitted via F and received by L apertures. For the MIMO system under consideration, it is assumed that the information bits are modulated using S-PSK and transmitted through the F apertures using repetition coding [34]. Thus, the received block of symbols at the lth receive aperture is given by

$$r_l\left[k\right] = \frac{\eta\mu P\sqrt{E_g}s\left[k\right]}{FL} \sum_{f=1}^{F} I^{(fl)} + \frac{1}{\sqrt{L}} n\left[k\right],\ k = 1, ..K \tag{41}$$

where $I^{(fl)}$ denotes the fading coefficient that models the atmospheric turbulence through the optical channel between the fth transmit and the lth receive aperture, while $n\left[k\right]$ represents AWGN with $\mathbb{E}\left\{n\left[k\right]n^*\left[k\right]\right\} = 2\sigma_n^2$. After adding the optical signals received from the L receive apertures (equal gain combining), the output of the receiver will be obtained as

$$r\left[k\right] = \sum_{l=1}^{L} r_l\left[k\right] = \frac{\eta\mu P\sqrt{E_g}s\left[k\right]}{FL} \sum_{f=1}^{F}\sum_{l=1}^{L} I^{(fl)} + n\left[k\right]. \tag{42}$$

Note that the factor F is included n (41) and (42), in order to ensure that the total transmit power is the same with that of a system with no transmit diversity, while the factor L ensures that the sum of the L receive aperture areas is the same with the aperture area of a system with no receive diversity. Moreover, the statistics of the fading coefficients of the underlying FSO links are considered to be statistically independent; an assumption which is realistic by placing the transmitter and the receiver apertures just a few centimeters apart [27].

The variable rate subcarrier PSK transmission scheme can be directly applied to the MIMO configuration with the decision on the modulation order to be based on

$$I_T = \frac{\sum_{f=1}^{F}\sum_{l=1}^{L} I^{(fl)}}{FL}. \tag{43}$$

Hence, after determining the region boundaries for the target P_o requirement, using Eqs. (25)-(27), the optimum modulation order will be selected from the N available ones depending on the value of I_T, i.e.,

$$M = M_j \text{ if } I_j \le I_T < I_{j+1},\ j = 1, ...N \tag{44}$$

Proposition 1: The achievable spectral efficiency of a MIMO adaptive S-PSK FSO system with F transmit and L receive apertures in LN turbulence induced fading, can be approximated by

$$S = \frac{\sum_{j=1}^{N} Q\left(y_j\right)}{2} \tag{45}$$

with $y_j = \frac{\ln(I_j)+\frac{1}{2}\sigma_\xi^2}{\sigma_\xi}$ and $\sigma_\xi^2 = \ln\left(1 + \frac{e^{4\sigma_x^2}-1}{FL}\right)$.

Proof: The proof follows trivially by recalling that the PDF of I_T in LN turbulence induced fading can be efficiently approximated by [11], [27]

$$I_T = \exp\left(\xi\right) \tag{46}$$

where $f_\xi(\xi) = \mathcal{N}\left(m_\xi, \sigma_\xi^2\right)$, $\sigma_\xi^2 = \ln\left(1 + \frac{e^{4\sigma_x^2}-1}{FL}\right)$ and $m_\xi = -\frac{1}{2}\sigma_\xi^2$. Hence, using (32), the achievable spectral efficiency of the MIMO adaptive FSO system will be approximated by (45). ■

Proposition 2: The achievable spectral efficiency of a MIMO adaptive S-PSK FSO system with F transmit and L receive apertures in GG turbulence induced fading, can be approximated by

$$S = \frac{N}{2} - \frac{1}{2\Gamma(\alpha_T)\Gamma(\beta_T)} \sum_{j=1}^{N} G_{1,3}^{2,1}\left[z_j \left| \begin{array}{c} 1 \\ \alpha_T, \beta_T, 0 \end{array} \right. \right] \quad (47)$$

where $z_j = \alpha_T \beta_T I_j$, $\alpha_T = FLa + \varepsilon$, $\beta_T = FLb$, $a = \max(\alpha, \beta)$, $b = \min(\alpha, \beta)$ and

$$\varepsilon = (FL-1)\frac{-0.0127 - 0.95a - 0.0058b}{1 + 0.124a + 0.98b}. \quad (48)$$

Proof: By applying the approximation for the sum of i.i.d. GG variates derived in [35], the PDF of I_T can be approximated by

$$f_{I_T}(I) = \frac{2\left(\frac{\alpha_T\beta_T}{FL}\right)^{\frac{\alpha_T+\beta_T}{2}}}{\Gamma(\alpha_T)\Gamma(\beta_T)} I^{\frac{\alpha_T+\beta_T-2}{2}} K_{a_T-\beta_T}\left(2\sqrt{\alpha_T\beta_T I}\right) \quad (49)$$

where $\alpha_T = FL\max(\alpha,\beta) + \varepsilon$, $\beta_T = L\min(\alpha,\beta)$ and ε is the approximation error given by (48). Hence, the CDF of I_T can be derived, using [36, Eq. (26)], as

$$F_{I_T}(I_{th}) = \frac{1}{\Gamma(\alpha_T)\Gamma(\beta_T)} G_{1,3}^{2,1}\left[\alpha_T\beta_T I_{th} \left| \begin{array}{c} 1 \\ \alpha_T, \beta_T, 0 \end{array} \right. \right] \quad (50)$$

and, therefore, the achievable spectral efficiency, according to (32) is given by (47). ■

Furthermore, the average BER of the adaptive MIMO FSO system will be obtained by

$$\bar{P}_b = \frac{\sum_{j=1}^{N+1} \langle P_b \rangle_j \log_2 M_j}{\sum_{j=1}^{N+1} v_j \log_2 M_j} \quad (51)$$

where

$$\langle P_b \rangle_j = \int_{I_j}^{I_{j+1}} P_b(M_j, I) f_{I_T}(I)\, dI \quad (52)$$

and

$$u_j = \Pr\{I_j \le I_T < I_{j+1}\} = F_{I_T}(I_{j+1}) - F_{I_T}(I_j). \quad (53)$$

To the best of the authors' knowledge it is difficult to derive analytical expressions for the above equations, either when LN or GG turbulence induced fading model is considered. Therefore, numerical methods need to be employed for their evaluation.

IV. Results & Discussion

In this section, we present numerical results for the performance of the adaptive S-PSK scheme in various turbulence conditions and fading models, and for different target BERs. We further apply this transmission policy to different MIMO deployments.

Figs. 1-4 depict the spectral efficiency of the adaptive S-PSK transmission scheme at different degrees of turbulence

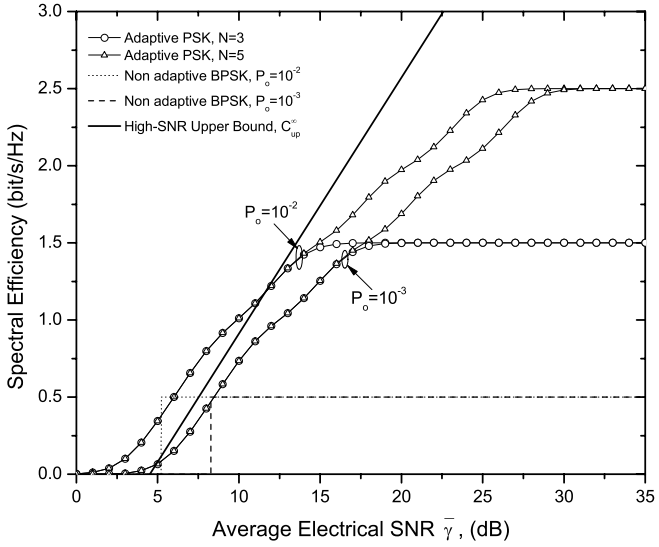

Fig. 1. Spectral efficiency of the adaptive subcarrier PSK scheme when LN fading model is considered and $\sigma_I^2 = 0.04$ ($\sigma_x = 0.1$).

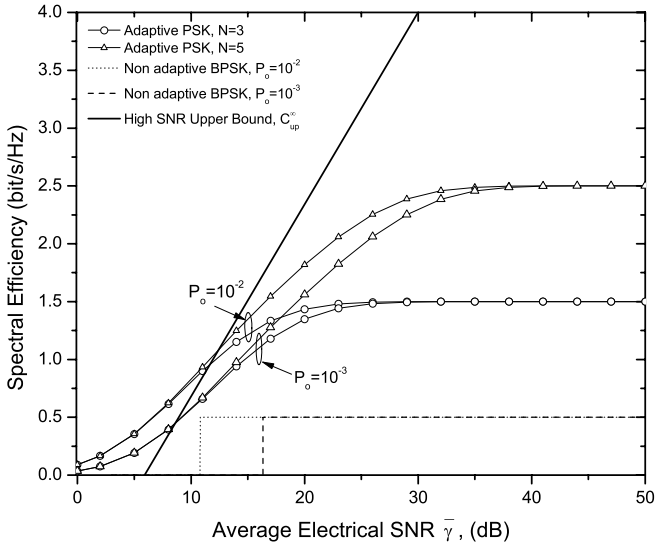

Fig. 2. Spectral efficiency of the adaptive subcarrier PSK scheme when LN fading model is considered and $\sigma_I^2 = 0.43$ ($\sigma_x = 0.3$).

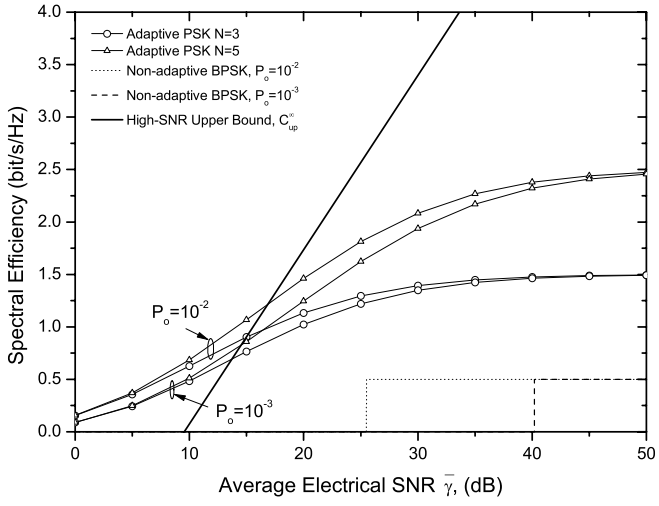

Fig. 3. Spectral efficiency of the adaptive subcarrier PSK scheme when GG fading model is considered and $\sigma_I^2 = 1.39$ ($\alpha = 2.23,\ \beta = 1.54$).

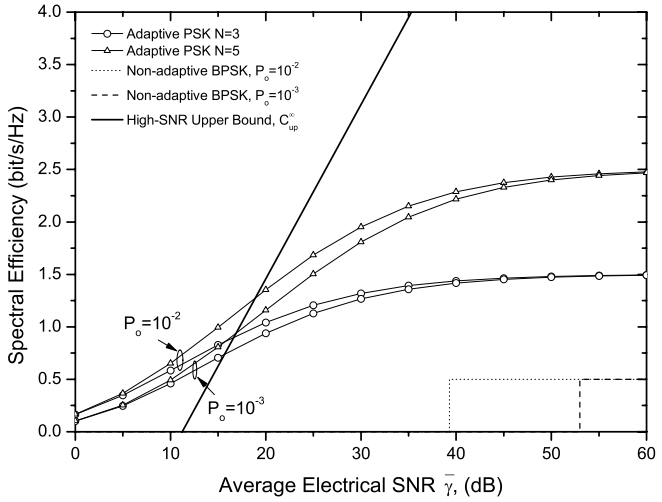

Fig. 4. Spectral efficiency of the adaptive subcarrier PSK scheme when GG fading model is considered and $\sigma_I^2 = 1.82$ ($\alpha = 2.34,\ \beta = 1.02$).

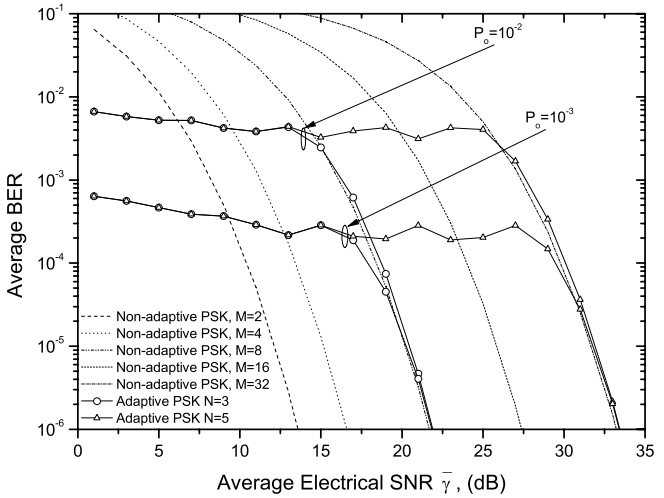

Fig. 5. Average BER of the adaptive subcarrier PSK scheme when LN fading model is considered and $\sigma_I^2 = 0.04$ ($\sigma_x = 0.1$).

strength, i.e., $\sigma_I^2 = 0.04$, $\sigma_I^2 = 0.43$, $\sigma_I^2 = 1.39$ and $\sigma_I^2 = 1.82$, and when a SISO FSO system is considered. Specifically, numerical results obtained either by (33) or (36), depending on the fading model employed for turbulence description, are plotted as a function of the average electrical SNR, $\bar{\gamma}$, for two different target BER requirements, $P_o = 10^{-2}$ and $P_o = 10^{-3}$. Furthermore, in the same figures, the upper bound, provided by (19), along with the spectral efficiency of the non-adaptive subcarrier BPSK ($M = 2$) are illustrated. The latter is found by determining the value of the average electrical SNR for which the BER performance of the non-adaptive BPSK, as given by (13) and (15) for LN and GG turbulence fading models respectively, equals P_o. It is obvious from the figures that the spectral efficiency of the adaptive transmission scheme increases and comes closer to the upper channel capacity bound by increasing the target P_o. Moreover, when compared to the non-adaptive BPSK, it is observed that adaptive transmission offers large spectral efficiency gains (42dB when $P_o = 10^{-3}$) at strong turbulence conditions ($\sigma_I^2 = 1.82$); however, these gains are reduced as σ_I^2 reduces. For very low turbulence ($\sigma_I^2 = 0.04$), it is observed that non-adaptive BPSK reached its maximum spectral efficiency ($S = 0.5$) at lower values of $\bar{\gamma}$ than the proposed adaptive scheme, indicating that in these turbulence conditions, it is more efficient to modify the modulation order based on $\bar{\gamma}$ rather than the instantaneous value of fading intensity.

Figs. 5-8 illustrate the average BER performance of the adaptive transmission technique for the same target BER requirements and turbulence conditions. It is clearly depicted that the average BER of the adaptive system is lower than the target P_o in all cases examined, satisfying the basic design requirement of (23). Moreover, it can be easily observed from Figs. 5-6 that the performance of the adaptive system approaches the performance of the non-adaptive system with the largest modulation order, at high values of average SNR; this was expected, since in this SNR regime the adaptive scheme chooses to transmit with the largest available modulation order.

Finally, Figs. 9-10 depict numerical results for the spectral efficiency of various MIMO FSO deployments and for differ-

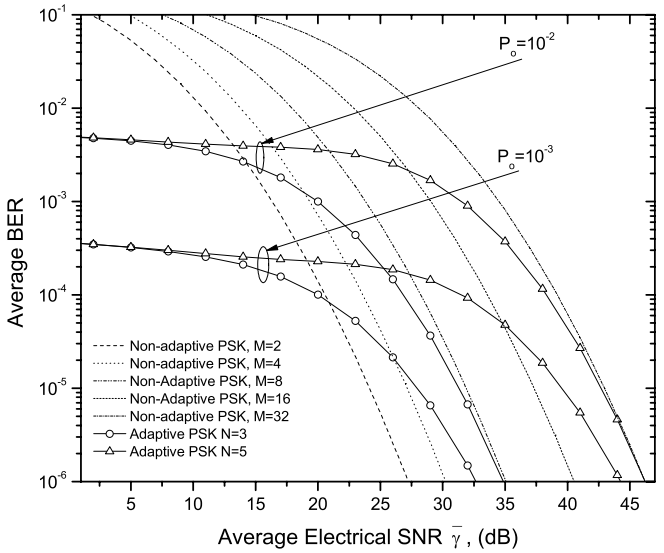

Fig. 6. Average BER of the adaptive subcarrier PSK scheme when LN fading model is considered and $\sigma_I^2 = 0.43$ ($\sigma_x = 0.3$).

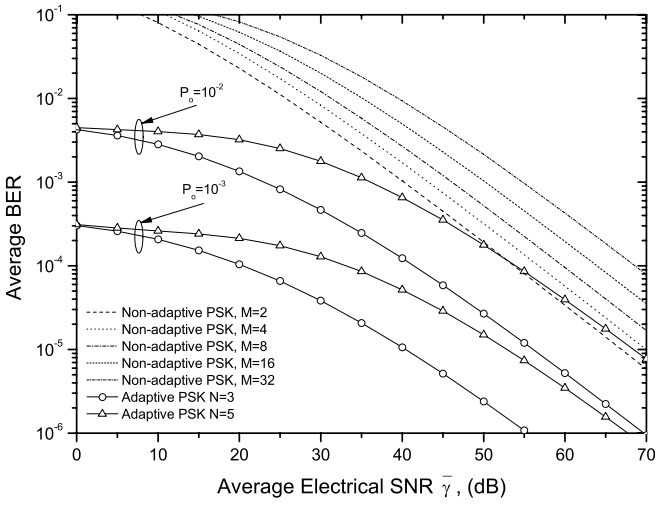

Fig. 7. Average BER of the adaptive subcarrier PSK scheme when GG fading model is considered and $\sigma_I^2 = 1.39$ ($\alpha = 2.23,\ \beta = 1.54$).

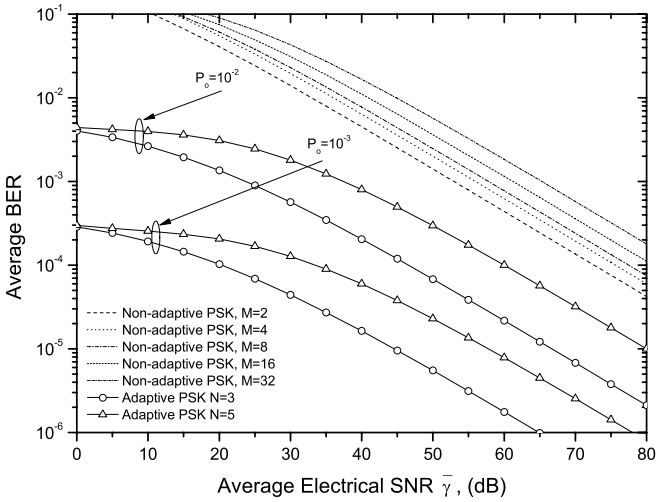

Fig. 8. Average BER of the adaptive subcarrier PSK scheme when GG fading model is considered and $\sigma_I^2 = 1.82$ ($\alpha = 2.34,\ \beta = 1.02$).

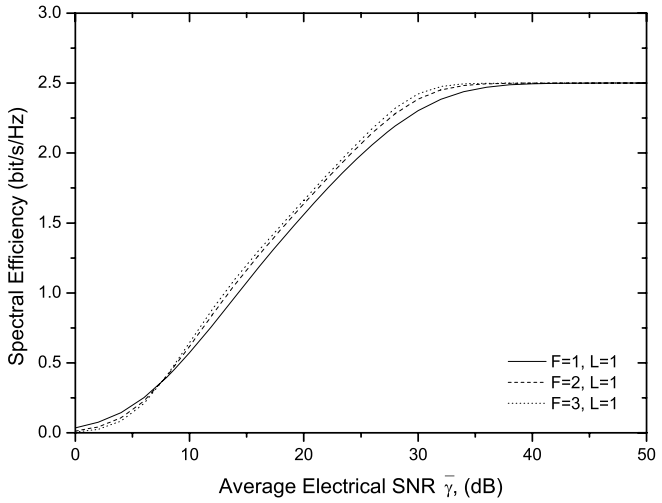

Fig. 9. Spectral efficiency of the adaptive subcarrier PSK scheme for various MIMO configurations, when LN fading model is considered and $N = 5$, $P_o = 10^{-3}$, $\sigma_I^2 = 0.43$ ($\sigma_x = 0.3$).

ent fading models, when the adaptive transmission technique with target $P_o = 10^{-3}$ and $N = 3$ available modulation orders is applied. As it is clearly illustrated in both figures, the increase of the number of transmit and/or receive apertures improves the performance of the adaptive transmission scheme, increasing the achievable spectral efficiency. However, this does not happen at low values of average SNR (less than 8dB), which may seem surprising at first but can be explained by the following argument. At the low average SNR regime, most of the region boundaries $\{I_j\}$ correspond to values higher than the unity. Hence, as the number of transmit and/or receive apertures increases, the parameters $\{F_{I_T}(I_j)\}$ also increase, resulting in less spectral efficiency. As the average SNR increases, most of the region boundaries $\{I_j\}$ take values lower than unity and, as a consequence, the increase in the number of apertures results in lower values for $\{F_{I_T}(I_j)\}$ and, thus, higher spectral efficiency.

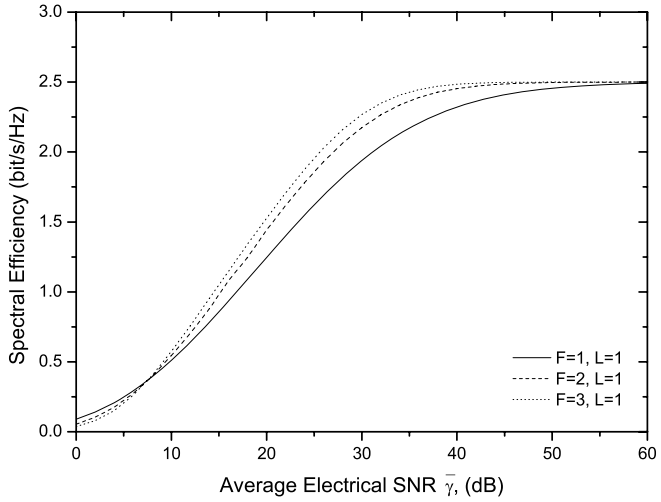

Fig. 10. Spectral efficiency of the adaptive subcarrier PSK scheme for various MIMO configurations, when GG fading model is considered and $N = 5$, $P_o = 10^{-3}$, $\sigma_I^2 = 1.38$ ($\alpha = 2.23,\ \beta = 1.54$).

V. Conclusions

We have presented a novel adaptive transmission technique for FSO systems operating in atmospheric turbulence and employing S-PSK intensity modulation. The described technique was implemented through the modification of the modulation order of S-PSK according to the instantaneous fading state and a pre-defined BER requirement. Novel expressions for the spectral efficiency and average BER of the adaptive FSO system were derived and investigations over various turbulence conditions, fading models and target BER requirements were performed. Numerical results indicated that adaptive transmission offers significant spectral efficiency gains, compared to the non-adaptive modulation, especially at the moderate-to-strong turbulence regime (42dB at $S = 0.5$, when $P_o = 10^{-3}$ and $\sigma_I^2 = 1.82$); however, it was observed that in very low turbulence ($\sigma_I^2 < 0.1$), it is more efficient to perform adaptation based on the average electrical SNR, instead of the instantaneous fading state. Furthermore, the proposed technique was applied at MIMO FSO systems and additional improvement in the achieved spectral efficiency was observed at the high SNR regime, as the number of the transmit and/or receive apertures increased.

Appendix

This appendix provides the proof for the derivation of (20). Using the PDF of LN turbulence induced fading, (19) can be written as

$$C_{up}^{\infty} = \frac{W}{4\sqrt{2\pi\sigma_x^2}} \int_0^{\infty} \frac{\log_2\left(\frac{\bar{\gamma} I^2}{e}\right)}{I} \exp\left(-\frac{\left(\ln I + 2\sigma_x^2\right)^2}{8\sigma_x^2}\right) dI \tag{54}$$

To simplify (54), we substitute $\ln I$ by y and hence

$$C_{up}^{\infty} = K_1 + K_2 \tag{55}$$

where

$$K_1 = \frac{W}{4\sqrt{2\pi\sigma_x^2}} \log_2\left(\frac{\bar{\gamma}}{e}\right) \int_{-\infty}^{\infty} \exp\left(-\frac{\left(y + 2\sigma_x^2\right)^2}{8\sigma_x^2}\right) dy \tag{56}$$

and

$$K_2 = \frac{W}{2\ln 2\sqrt{2\pi\sigma_x^2}} \int_{-\infty}^{\infty} y \exp\left(-\frac{\left(y+2\sigma_x^2\right)^2}{8\sigma_x^2}\right) dy. \quad (57)$$

Using [29, Eq. (3.321/3)], (56) is reduced to

$$K_1 = \frac{W}{2}\log_2\left(\frac{\bar{\gamma}}{e}\right) \quad (58)$$

while, using [29, Eq. (3.461/2)], (57) is reduced to

$$K_2 = -\frac{2W\sigma_x^2}{\ln 2}. \quad (59)$$

Hence, by combining (58) and (59) with (55), (20) is obtained.

REFERENCES

[1] L. Andrews, R. L. Philips, and C. Y. Hopen, *Laser Beam Scintillation with Applications*. SPIE Press, 2001.

[2] D. Kedar and S. Arnon, "Urban optical wireless communications networks: the main challenges and possible solutions," *IEEE Commun. Mag.*, vol. 42, no. 5, pp. 2-7, Feb. 2003.

[3] V. W. S. Chan, "Free-space optical communications," *J. Lightw. Technol.*, vol. 24, no. 12, pp. 4750-4762, Dec. 2006.

[4] S. Karp, R. Gagliardi, S. E. Moran, and L. B. Stotts, *Optical Channels*. Plenum, 1988.

[5] X. Zhu and J. M. Kahn, "Performance bounds for coded free-space optical communications through atmospheric turbulence channels," *IEEE Trans. Commun.*, vol. 51, no. 8, pp. 1233-1239, Aug. 2003.

[6] M. Uysal, S. M. Navidpour, and J. Li, "Error rate performance of coded free-space optical links over strong turbulence channels," *IEEE Commun. Lett.*, vol. 8, no. 10, pp. 635-637, Oct. 2004.

[7] X. Zhu and J. M. Kahn, "Free-space optical communication through atmospheric turbulence channels," *IEEE Trans. Commun.*, vol. 50, no. 8, pp. 1293-1300, Aug. 2002.

[8] M. L. B. Riediger, R. Schober, and L. Lampe, "Fast multiple-symbol detection for free-space optical communications," *IEEE Trans. Commun.*, vol. 57, no. 4, pp. 1119-1128, Apr. 2009.

[9] ——, "Reduced-complexity multiple-symbol detection for free-space optical communications," in *Proc. IEEE Global Commun. Conf.*, 2007, pp. 4548-4553.

[10] ——, "Blind detection of on-off keying for free-space optical communications," in *VCCECE/CCGEI*, 2008, pp. 1361-1364.

[11] S. M. Navidpour and M. Uysal, "BER performance of free-space optical transmission with spatial diversity," *IEEE Trans. Wireless Commun.*, vol. 6, no. 8, pp. 2813-2819, Aug. 2007.

[12] T. A. Tsiftsis, H. G. Sandalidis, G. K. Karagiannidis, and M. Uysal, "Optical wireless links with spatial diversity over strong atmospheric turbulence channels," *IEEE Trans. Wireless Commun.*, vol. 8, no. 2, pp. 951-957, Feb. 2009.

[13] M. S. Alouini and A. J. Goldsmith, "Adaptive moulation over Nakagami fading channels," *Wireless Personal Commun.*, vol. 13, no. 1-2, pp. 119-143, May 2000.

[14] A. Goldsmith, *Wireless Communications*. Cambridge University Press, 2005.

[15] B. K. Levitt, "Variable rate optical communication through the turbulent atmosphere," Technical Report 483, Massachusetts Institute of Technology, Research Laboratory of Electronics, Aug. 1971. Available: http://hdl.handle.net/1721.1/4260

[16] J. Li and M. Uysal, "Achievable information rate for outdoor free space optical communication with intensity modulation and direct detection," in *Proc. IEEE Global Commun. Conf.*, Nov. 2003, pp. 827-831.

[17] M. Gubergrits, R. Goot, U. Mahlab, and S. Arnon, "Adaptive power control for satellite to ground laser communication," *Int. J. Satellite Commun. Netw.*, vol. 25, no. 4, pp. 323-348, Aug. 2007.

[18] I. B. Djordjevic, "Adaptive modulation and coding for free-space optical channels," *IEEE/OSA J. Optical Commun. Netw.*, vol. 2, no. 5, pp. 221-229, May 2010.

[19] Q. Lu, Q. Liu, and G. S. Mitchell, "Performance analysis for optical wireless communication systems using sub-carrier PSK intensity modulation through turbulent atmospheric channel," in *Proc. IEEE Global Commun. Conf.*, 2004, p. 1872-1875.

[20] Q. Liu and Q. Li, "Subcarrier PSK intensity modulation for optical wireless communications through turbulent atmospheric channel," in *Proc. IEEE Int. Conf. Commun.*, 2005, p. 1761-1765.

[21] J. Li, J. Q. Liu, and D. P. Taylor, "Optical communication using subcarrier PSK intensity modulation through atmospheric turbulence channels," *IEEE Trans. Commun.*, vol. 55, no. 8, pp. 1598-1606, 2007.

[22] S. Arnon, "Minimization of outage probability of WiMAX link supported by laser link between a high-altitude platform and a satellite," *J. Optical Soc. Amer. A*, vol. 26, no. 7, pp. 1545-1552, July 2009.

[23] N. Cvijetic and T. Wang, "WiMAX over free-space optics–evaluating OFDM multi-subcarrier modulation in optical wireless channels," in *Proc. IEEE Sarnoff Symp.*, Mar. 2006, pp. 1-4.

[24] G. Katz, S. Arnon, P. Goldgeier, Y. Hauptman, and N. Atias, "Cellular over optical wireless networks," in *IEE Proc. Optoelectr.*, vol. 153, no. 4, pp. 195-198, Aug. 2006.

[25] R. You and J. M. Kahn, "Upper-bounding the capacity of optical IM/DD channels with multiple-subcarrier modulation and fixed bias using trigonometric moment space method," *IEEE Trans. Inf. Theory*, vol. 48, no. 2, pp. 514-523, Feb. 2002.

[26] D. J. T. Heatley, D. R. Wisely, I. Neild, and P. Cochrane, "Optical wireless: the story so far," *IEEE Commun. Mag.*, vol. 36, no. 2, pp. 72-74, Dec. 1998.

[27] E. Lee and V. Chan, "Part 1: optical communication over the clear turbulent atmospheric channel using diversity," *IEEE J. Sel. Areas Commun.*, vol. 22, no. 9, pp. 71,896-1906, Nov. 2004.

[28] N. Blaunstein, S. Arnon, N. Kopeika, and A. Zilberman, *Applied Aspects of Optical Communication and LIDAR*. Taylor and Francis/ CRC - Auerbach Publications, 2010.

[29] I. S. Gradshteyn and I. M. Ryzhik, *Table of Integrals, Series, and Products*, 7th edition. Academic, 2007.

[30] J. G. Proakis, *Digital Communications*, 4th edition. McGraw-Hill, 2000.

[31] M. Abramowitz and I. A. Stegun, *Handbook of Mathematical Functions with Formulas, Graphs, and Mathematical Tables*. Dover, 1970.

[32] A. P. Prudnikov, Y. A. Brychkov, and O. I. Marichev, *Integral and Series*. Gordon and Breach Science Publishers, 1986.

[33] T. A. Tsiftsis, "Performance of heterodyne wireless optical communication systems over gamma-gamma atmospheric turbulence channels," *Electron. Lett.*, vol. 44, no. 5, 2008.

[34] M. Safari and M. Uysal, "Do we really need space-time coding for free-space optical communication with direct detection?" *IEEE Trans. Wireless Commun.*, vol. 7, no. 11, pp. 4445-4448, Nov. 2008.

[35] N. D. Chatzidiamantis, G. K. Karagiannidis, and D. S. Michalopoulos, "On the distribution of the sum of Gamma-Gamma variates and application in MIMO optical wireless systems," in *Proc. EEE Global Commun. Conf.*, 2009.

[36] V. S. Adamchik and O. I. Marichev, "The algorithm for calculating integrals of hypergeometric type functions and its realization in REDUCE system," in *Proc. International Conf. Symbolic Algebraic Computation*, 1990, pp. 212-224.

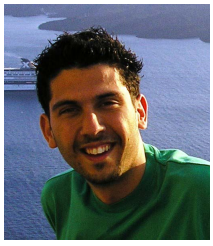

Nestor D. Chatzidiamantis (S'08) was born in Los Angeles, USA, in 1981. He received the Diploma degree (five years) in Electrical and Computer Engineering from the Aristotle University of Thessaloniki, Greece, and the M.Sc. award (with Distinction) in Telecommunication Networks and Software from the University of Surrey, U.K. in 2005 and 2006, respectively. In November 2007, he joined again the ECE department of the Aristotle University of Thessaloniki, where he is pursuing a Ph.D. degree.

His research areas span performance analysis of wireless communication systems over fading channels, communications theory and free-space optical communications.

Athanasios S. Lioumpas was born in Thessaloniki, Greece, in 1982. He received his diploma in 2005 and his Ph.D. degree in 2009, both in Electrical Engineering, from the Aristotle University of Thessaloniki, Greece.

In 2010, he joined the University of Piraeus, Greece, where he is currently a Post-Doctoral Researcher at the Department of Digital Systems.

His current research interests include digital communications over fading channels, machine-to-machine and next-generation wireless communications. He has published more than 20 refereed journal/conference articles and holds four patents.

Dr. Lioumpas is co-recipient of the Best Paper Award of the Wireless Communications Symposium (WCS) in IEEE International Conference on Communications (ICC'07), Glasgow, U.K., June 2007.

George K. Karagiannidis (M'97-SM'04) was born in Pithagorion, Samos Island, Greece. He received the University Diploma (five years) and Ph.D. degree, both in electrical and computer engineering, from the University of Patras, in 1987 and 1999, respectively. From 2000 to 2004, he was a Senior Researcher at the Institute for Space Applications and Remote Sensing, National Observatory of Athens, Greece. In June 2004, he joined Aristotle University of Thessaloniki, Thessaloniki, where he is currently an Associate Professor of Digital Communications Systems in the Electrical and Computer Engineering Department and Head of the Telecommunications Systems and Networks Lab.

His current research interests are in the broad area of digital communications systems with emphasis on cooperative communication, adaptive modulation, MIMO systems, optical wireless and underwater communications.

He is the author or co-author of more than 120 technical papers published in scientific journals and presented at international conferences. He is also a co-author of three chapters in books and author of the Greek edition book on Telecommunications Systems.

Dr. Karagiannidis has been a member of Technical Program Committees for several IEEE conferences as ICC, GLOBECOM, etc. He is a member of the editorial board of the IEEE TRANSACTIONS ON COMMUNICATIONS, Senior Editor of the IEEE COMMUNICATIONS LETTERS, and Lead Guest Editor of the special issue on "Optical Wireless Communications" of the IEEE JOURNAL ON SELECTED AREAS IN COMMUNICATIONS. He is co-recipient of the Best Paper Award of the Wireless Communications Symposium (WCS) in IEEE International Conference on Communications (ICC'07), Glasgow, U.K., June 2007.

Dr. Karagiannidis is the Chair of the IEEE COMSOC Greek Chapter.

Shlomi Arnon is a faculty member in the Department of Electrical and Computer Engineering at Ben-Gurion University (BGU), Israel. There, in 2000, he established the Satellite and Wireless Communication Laboratory which has been under his directorship since then. During 1998-1999 Professor Arnon was a Postdoctoral Associate (Fullbright Fellow) at LIDS, Massachusetts Institute of Technology (MIT), Cambridge, USA. His research has produced more than 50 journal papers in the area of satellite, optical and wireless communication. During part of the summer of 2007, he worked at TU/e and Philips LAB, Eindhoven, Netherland on a novel concept of a dual communication and illumination system. He was visiting professor during the summer of 2008 at TU Delft, Netherland. He is SPIE Fellow. Professor Arnon is a frequent invited speaker and program committee member at major IEEE and SPIE conferences in the US and Europe. He was an associate editor for the Optical Society of America - *Journal of Optical Networks*, on a special issue on optical wireless communication that appeared in 2006, and on the editorial board for the IEEE JOURNAL ON SELECTED AREAS IN COMMUNICATIONS for a special issue on optical wireless communication. 2009. Professor Arnon continuously takes part in many national and international projects (for example with NASA LUNAR science Institute) in the areas of satellite communication, remote sensing, cellular and mobile wireless communication. He consults regularly with start-up and well-established companies in the area of optical, wireless and satellite communication. In addition to research, Professor Arnon and his students work on many challenging engineering projects with especial emphasis on the humanitarian dimension. For instance, a long-standing project has dealt with developing a system to detect human survival after earthquakes, or Infant respiration monitoring system to prevent cardiac arrest and Apnea or Detection of falls in the case of epilepsy sufferers and elderly people.